Numerical evaluation of the gradient of the inter-quark potential

Yoshiaki KOMA*

The inter-quark potential computed by lattice QCD Monte Carlo simulations contains valuable information on the nonperturbative dynamics of quarks and gluons in quantum chromodynamics, which is relevant to the understanding of the hadron structures. We investigate the functional form of the potential in detail not only by applying the χ^2 fitting but also by evaluating the gradient of the potential, and clarify its behavior as a function of the inter-quark distance.

I. INTRODUCTION

Recently, we have computed the potential energy for the various quark systems, the inter-quark potential, by performing large scale numerical simulations of QCD using the discrete lattice formulation in four-dimensional Euclidean space-time (lattice QCD Monte Carlo simulations) [1–3]. QCD is an abbreviation of the quantum gauge field theory associated with the SU(3) group symmetry called "quantum chromodynamics" discovered in the 1970s [4], which is supposed to describe the dynamics of quarks and gluons inside mesons and baryons, i.e., hadrons. We then confront with the problem of finding the appropriate functional form of the inter-quark potential, which is relevant to the understanding of the hadron structures.

Given a set of experimental data, one often summarizes its behavior by fitting it to a model function with adjustable parameters. The χ^2 fitting is widely used for this purpose. For the set of discrete data point (x_i, y_i) $(i = 1, 2, ..., n_p)$ with the standard deviation σ_i the model function $y_{\rm fit}$ is assumed to be a function of x with a set of parameters $\vec{a} = (a_1, a_2, ..., a_{n_{\rm para}})$, which is determined so as to minimize the value of χ^2 defined by

$$\chi^2 = \sum_{i=1}^{n_{\rm p}} \left(\frac{y_i - y_{\rm fit}(x_i; \vec{a})}{\sigma_i} \right)^2 . \qquad (1)$$

Depending on the value of χ^2, one argues the goodness of the fitting and the validity of the model function. If the fitting works well, the value of $\chi^2/n_{\rm df}$, where $n_{\rm df} = n_{\rm p} - n_{\rm para}$, will be of $O(1)$.

The χ^2 fitting can then be applied for the determination of the functional form of the inter-quark potential, since the results are given by a set of numerical values associated with the statistical errors. However, a weakness of the χ^2 fitting may be that the model function cannot be selected uniquely only by looking at the value of χ^2. If there exists an analytical prediction from QCD on the behavior of the inter-quark potential, the obtained functional form can be used to examine the validity of QCD, but this is not the case in QCD due to its nonperturbative nature, and this is the reason why we have resorted to numerical simulations.

In this report, we investigate the functional form of the inter-quark potential by applying not only the χ^2 fitting but also the additional method so as to compensate the weakness of the χ^2 fitting. In particular, we look at the gradient of the inter-quark potential, that is, the derivative of the potential with respect to the distance between quarks. We note, however, that this additional method is applicable only when the numerical errors of the original data are highly suppressed, otherwise the gradient will be noisy and relevant information will be obscured. The numerical data of our simulations satisfy this criterion by virtue of the simulation algorithm called the multi-level algorithm [5, 6].

II. NUMERICAL PROCEDURES

We perform lattice QCD simulations within the quenched approximation in four dimensions with the lattice volume $L^3 \times T$ and the lattice spacing a by imposing periodic boundary conditions in all space-time directions. The inter-quark potential is extracted from the expectation value of the Polyakov loop correlation function (PLCF). In what follows we only explain how to compute the inter-quark potential for the quark-antiquark system (mesons), but the similar procedure is also applicable to the three-quark system (baryons).

*Division of Liberal Arts / Physics group

We define a two-link correlator as

$$\mathbb{T}(t,\vec{r}_1,\vec{r}_2)_{\alpha\beta\gamma\delta} \equiv U_4(t,\vec{r}_1)_{\alpha\beta}U_4(t,\vec{r}_2)^*_{\gamma\delta} \ , \qquad (2)$$

which is a direct product of two temporal link variables at a time t separated by a distance $r=|\vec{r}_1-\vec{r}_2|$ and consists of a complex matrix with $3^4 = 81$ components (Greek indices take the values from 1 to 3). The spatial vectors $\vec{r}_1$ and $\vec{r}_2$ represent the spatial positions of a quark and an antiquark, respectively. The two-link correlator acts on the color states in the $\mathbf{3}\otimes\bar{\mathbf{3}}$ representation of the SU(3) group $|n;\vec{r}_1,\vec{r}_2\rangle_{\alpha\beta}$, which satisfies $\mathbb{T}(t,\vec{r}_1,\vec{r}_2)_{\alpha\lambda\gamma\epsilon}|n;\vec{r}_1,\vec{r}_2\rangle_{\alpha\gamma} = e^{-E_n(r)a}|n;\vec{r}_1,\vec{r}_2\rangle_{\lambda\epsilon}$, where n is the principal quantum number (repeated indices are assumed to be summed over from 1 to 3). The energies $E_n(r)$ are positive, which are common to all color components of $|n;\vec{r}_1,\vec{r}_2\rangle_{\alpha\beta}$. The multiplication rule of the two-link correlators for the two neighboring time at t and $t+a$ is

$$\begin{aligned}&\{\mathbb{T}(t,\vec{r}_1,\vec{r}_2)\mathbb{T}(t+a,\vec{r}_1,\vec{r}_2)\}_{\alpha\beta\gamma\delta}\\ &= \mathbb{T}(t,\vec{r}_1,\vec{r}_2)_{\alpha\lambda\gamma\epsilon}\mathbb{T}(t+a,\vec{r}_1,\vec{r}_2)_{\lambda\beta\epsilon\delta} \ . \end{aligned} \qquad (3)$$

By using the two-link correlators, the PLCF is then constructed as

$$\begin{aligned}&\mathrm{Tr}P(\vec{r}_1)\mathrm{Tr}P(\vec{r}_2)^*\\ &= \{\mathbb{T}(0,\vec{r}_1,\vec{r}_2)\mathbb{T}(a,\vec{r}_1,\vec{r}_2)\cdots\mathbb{T}(T-a,\vec{r}_1,\vec{r}_2)\}_{\alpha\alpha\gamma\gamma} \ . \end{aligned} \qquad (4)$$

The expectation value is evaluated by inserting the complete set of eigenstates at all times $t = 0, a, ..., T-a$ as

$$\langle \mathrm{Tr}P(\vec{r}_1)\mathrm{Tr}P(\vec{r}_2)^*\rangle = \sum_{n=0}^{\infty} w_n e^{-E_n(r)T} \ , \qquad (5)$$

where $w_0 = 1$ is guaranteed automatically. We finally obtain the ground state potential $V(r) \equiv E_0(r)$ by

$$V(r) = -\frac{1}{T}\ln\langle \mathrm{Tr}P(\vec{r}_1)\mathrm{Tr}P(\vec{r}_2)^*\rangle + O(e^{-(E_1-E_0)T}), \qquad (6)$$

where the terms of $O(e^{-(E_1-E_0)T})$ are always negligible at zero temperature. Although it is impossible to compute the expectation values of the PLCF accurately within the ordinary simulations as they are extremely small at long distances, it is possible to overcome this problem by using the multi-level algorithm.

The idea of the multi-level algorithm is to compute the correlation function, which may have an extremely small expectation value, from the product of relatively large sub-lattice averages of its components (in our case it corresponds to the product of $\mathbb{T}$s within a sub-lattice), where the sub-lattice is defined by dividing the lattice volume into several layers along the time direction. During the computation of the sub-lattice averages, the spatial links at the sub-lattice boundaries are kept intact. The computation of the correlation function in this way is supported by the transfer matrix formalism of quantum field theory.

III. NUMERICAL RESULTS

We carried out lattice QCD simulations using the standard Wilson gauge action at the coupling $\beta = 6.00$ on the $L^3 \times T = 24^3 \times 24$ lattice with the multi-level algorithm. The lattice spacing $a = 0.093\,[\mathrm{fm}]$, which is determined by the Sommer scale $r_0 = 0.50\,[\mathrm{fm}]$ [7]. One Monte Carlo update consisted of one heat-bath and five over-relaxation steps. The number of sub-lattice $N_{\mathrm{sub}} = 6$, which corresponds to $N_{\mathrm{tsl}} = 4$, so that $aN_{\mathrm{tsl}} = 0.372\,[\mathrm{fm}]$. The number of internal updates $N_{\mathrm{iupd}} = 10000$ and the number of gauge configurations $N_{\mathrm{cnf}} = 200$. The numerical errors of the inter-quark potential and its derivatives are estimated by the jackknife method.

In Fig. 1, we plot the quark-antiquark potential as a function of the inter-quark distance r/a. We find that the most of the data fall into one curve. The labels (i,j,k) represent the base vectors along the quark-antiquark direction. For instance, the data belong to $(1,0,0)$ are for the case that the quark and antiquark are separated along the x, y, and z axes (on-axis), while the data belong to $(1,1,0)$, $(1,1,1)$, and $(2,1,0)$ are for the cases that the quark and antiquark are separated along the off-axis. The unit Euclidean distances for these off-axis settings are $r/a = \sqrt{2}$, $\sqrt{3}$, and $\sqrt{5}$, respectively. Note that the tree-level improvement is applied to the inter-quark distance before plotting the data by using the three-dimensional Green's function in infinite volume, which helps to reduce the lattice discretization effect [7]. The dotted line is the model function in the form

$$V_{\mathrm{fit}}(r) = -\frac{c}{r} + \sigma r + \mu \ , \qquad (7)$$

which is fitted to the on-axis $(1,0,0)$ data. We obtain

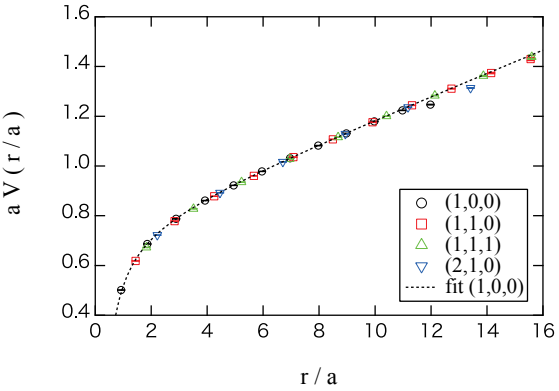

FIG. 1: The quark-antiquark potential as a function of the inter-quark distance r/a.

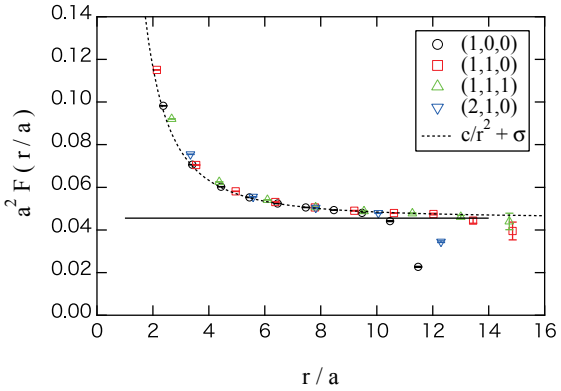

FIG. 2: The first derivative of the quark-antiquark potential with respect to the inter-quark distance r/a.

$c = 0.2826(7)$, $\sigma a^2 = 0.04558(7)$, and $\mu a = 0.7540(5)$ for the fitting range $r/a = 1.855 \sim 9.974$ (corresponding to $r/a = 2 \sim 10$ before the tree-level improvement) with $n_p = 9$ and $\chi^2 = 3.1$ ($\chi^2/n_{\rm df} = 0.52$). We call c the Coulombic coefficient, σ the string tension, and μ just a constant. We then find that the off-axis data behave nicely up to the distances longer than the half of the spatial lattice volume $r/a = 12$, at where the on-axis data already suffer from finite volume effects.

In order to confirm the validity of this functional form, we further investigate the gradient of the potential data. In Fig. 2, we plot the first derivative of the quark-antiquark potential with respect to the inter-quark distance r/a,

$$F(r+\frac{h}{2}) = \frac{V(r+h)-V(r)}{h} \ , \tag{8}$$

where $h/a = 1$ for the on-axis $(1,0,0)$ data, and $h/a = \sqrt{2}$, $\sqrt{3}$, $\sqrt{5}$ for the off-axis $(1,1,0)$, $(1,1,1)$, $(2,1,0)$ data, respectively. If the model function in Eq. (7) is valid, the first derivative F should behave as

$$\frac{dV_{\rm fit}}{dr} = \frac{c}{r^2} + \sigma \ . \tag{9}$$

The data seem to fall into this curve (dotted line) and approach the value $\sigma a^2 = 0.04558$ at long distances (solid line).

It is possible to extract the Coulombic coefficient c directly from the second derivative of the potential. For the model function in Eq. (7) its derivatives with respect to r behave as

$$V''_{\rm fit} = -\frac{2c}{r^3}, \ V^{(4)}_{\rm fit} = -\frac{4!c}{r^5}, \ V^{(6)}_{\rm fit} = -\frac{6!c}{r^7}, \ldots \ . \tag{10}$$

Therefore we expect

$$\begin{aligned} &\frac{V(r+h)+V(r-h)-2V(r)}{h^2} \\ &= V'' + 2\frac{h^2}{4!}f^{(4)} + 2\frac{h^4}{6!}f^{(6)} + \cdots \\ &= -\frac{2c}{r^3}(1+\frac{h^2}{r^2}+\frac{h^4}{r^4}+\cdots) \\ &= -\frac{2c}{r^3}(1-\frac{h^2}{r^2})^{-1} \ , \end{aligned} \tag{11}$$

and obtain

$$c = -\frac{r^3}{2}(1-\frac{h^2}{r^2})(\frac{V(r+h)+V(r-h)-2V(r)}{h^2}) \ . \tag{12}$$

The corresponding continuum expression derived from Eq. (7) is

$$c = -\frac{r^3}{2}V''_{\rm fit}(r) \ . \tag{13}$$

Note that the $O(h^2)$ terms present in the ordinary second difference is properly removed by the factor $(1-\frac{h^2}{r^2})$ in Eq. (12).

In Fig. 3, we plot the Coulombic coefficient c computed by Eq. (12) as a function of r/a. We find that the value of c is approximately constant around $c \simeq 0.3$. The two solid lines correspond to the $c = 0.282$ and $c = 0.315$, which are the minimum and the maximum values obtained by the χ^2 fitting of the potential for the on-axis and the off-axis settings. The values of c in the range $r/a = 3 \sim 8$ lie within these two lines. The deviation at long distances $r/a > 9$ is due to finite volume effects, which is expected to disappear for larger lattice volumes. If we consider the deviation at short distance $r/a < 3$ seriously, we may conclude that the term $-c/r$ in Eq. (7) is not enough

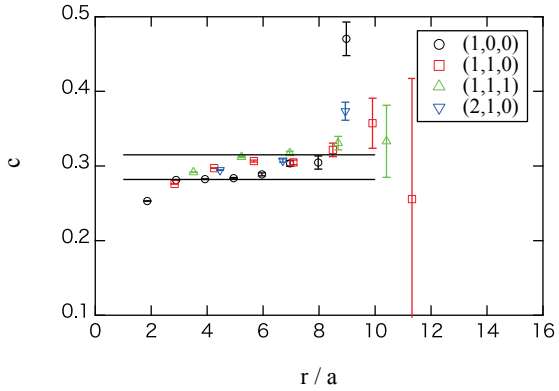

FIG. 3: The Coulombic coefficient c extracted from the second derivative of the potential.

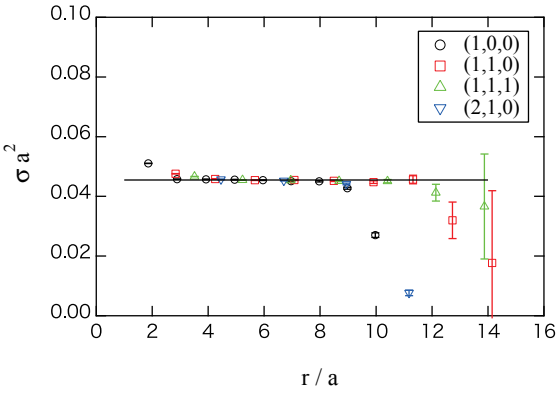

FIG. 4: The string tension σa^2 extracted from the second derivative of the potential after multiplying r.

to describe the short distance behavior of the potential. A possible explanation may be that the c is not constant but dependent on r. It is interesting to investigate the short distance behavior in detail, which however is beyond the scope of the present report.

In Fig. 4, we plot the string tension σa^2 directly extracted from the second derivative of the potential after multiplying r,

$$\sigma a^2 = \frac{1}{2}\frac{(r+h)V(r+h)+(r-h)V(r-h)-2rV(r)}{h^2} . \tag{14}$$

The corresponding continuum expression derived from Eq. (7) is

$$\sigma a^2 = \frac{1}{2}\frac{d^2}{dr^2}(rV_{\rm fit}(r)) . \tag{15}$$

We find that the values of σa^2 behave as constant, which lie on the solid line corresponding to the value $\sigma a^2 = 0.04558$ obtained by the χ^2 fitting. We then conclude that the linear-rising term is certainly present in the quark-antiquark potential. The deviation at long distances is due to finite volume effects, while the deviation at short distances indicates that there exist the terms which do not behave as constant even after multiplying r to the potential.

IV. SUMMARY

We have investigated the functional form of the inter-quark potential obtained by the lattice QCD simulations not only by applying the χ^2 fitting but also by evaluating the gradient of the potential. We have confirmed that the quark-antiquark potential can be described mostly by the sum of the Coulombic term and the linear term, which is actually the well-known result, but we have further clarified the r dependence of the Coulombic coefficient and the string tension. The results indicate that some modifications to the Coulombic term are needed for the perfect description of the potential including the data at short distances. We plan to apply similar analyses presented in this report to the determination of the functional form of the three-quark potential [1–3].

The author is grateful to Miho Koma (Nihon University) for fruitful collaboration. The computation was performed on the supercomputer NEC SX-ACE at Cybermedia Center, Osaka University. This work is partially supported by JSPS KAKENHI Grant Number 24740176.

[1] Y. Koma and M. Koma, *PoS* **LAT2013** (2013) 469.
[2] Y. Koma and M. Koma, *PoS* **LAT2014** (2014) 352.
[3] M. Koma and Y. Koma, *PoS* **LAT2015** (2015) 324.
[4] W. Greiner and A. Schäfer, "Quantum chromodynamics," Berlin, Germany: Springer (1994).
[5] M. Lüscher and P. Weisz, *JHEP* **09** (2001) 010.
[6] M. Lüscher and P. Weisz, *JHEP* **07** (2002) 049.
[7] S. Necco and R. Sommer, *Nucl. Phys.* **B622** (2002) 328.